J. RADIAT. RES., 41, 243–258 (2000)

UVC-induced Apoptosis in Human Epithelial Tumor A431 Cells: Sequence of Apoptotic Changes and Involvement of Caspase (–8 and –3) Cascade

KEUN HEE CHOI[1,2], HIROKO HAMA-INABA[1], BING WANG, KEIKO HAGINOYA[1], TAKEKO ODAKA[1], TAKESHI YAMADA[1], ISAMU HAYATA[1] and HARUMI OHYAMA[1]*

[1]Division of Radiobiology and Biodosimetry, National Institute of Radiological Sciences, Anagawa 4–9–1, Inage-ku, Chiba 263–8555, Japan
[2]Department of Cosmetology, Dongkang College, 771 Duamdong, Bukgu, Kwangju 500–714, Korea
(*Received, April 12, 2000*)
(*Revision received, June 23, 2000*)
(*Accepted, July 20, 2000*)

UVC-induced apoptosis/A431 cells/Apoptotic changes/Caspases/Caspase inhibitors

Human epidermoid tumor A431 cells underwent apoptosis following exposure to ultraviolet C (UVC). The apoptosis was of the interphase death type, and mostly occurred within one cell cycle, independent of the cell-cycle phases. We further examined the detailed sequential order of apoptotic changes in cells after UVC exposure and the involvement of caspases using six caspase inhibitors. The loss of mitochondrial transmembrane potential ($\Delta\Psi$m) appeared in the earliest phase; subsequently, the chromatin condensation and DNA-fragmentation occurred. Cell shrinkage and loss of the plasma-membrane integrity, judged by propidium iodide (PI) staining, were observed in the later phase. A broad-spectrum caspase inhibitor, z-VAD-fmk, completely prevented all apoptotic changes, except for the depletion of $\Delta\Psi$m. Both Ac-DEVD-CHO and Ac-IETD-CHO, inhibitors of caspase –3 and –8, respectively, effectively inhibited typical chromatin condensation to almost the same extent. However, the nuclei still showed partial condensation. A caspase –9 inhibitor, Ac-LEHD-CHO, did not prevent chromatin condensation, though it partially inhibited cell-size reduction and PI-stainability. None of the caspase inhibitors could inhibit the $\Delta\Psi$m reduction. These results strongly suggest that the collapse of $\Delta\Psi$m is not a part of the central apoptotic machinery, and that caspase cascade(s), especially caspase–8 to –3, play an important role in UVC-induced apoptosis in A431.

*Corresponding author: Phone; +81–43–206–3075, Fax; +81–43–255–6802, E-mail; ohyama@nirs.go.jp
Abbreviations: Z, benzyloxycarbonyl; Ac, acetyl; CHO, aldehyde; fmk, fluoromethylketone; VAD, Val-Ala-Asp; YVAD, Try-Val-Ala-Asp; DEVD, Asp-Glu-Val-Asp; VEID, Val-Glu-Ile-Asp; IETD, Ile-Glu-Thr-Asp; LEHD, Leu-Glu-His-Asp

INTRODUCTION

Apoptosis is induced by a wide variety of stresses, including ultraviolet light (UV) and ionizing radiation[1–3]. UV induces apoptosis in various cell types, including normal and malignant epithelial cells[1–5]. UVB (290–320 nm) and UVC (200–290 nm), especially UVC, induce mainly DNA damage, coupled with p53 phosphorylation, resulting in its accumulation in the nucleus and a subsequent induction of apoptosis, or G_1 arrest[6,7]. Mutations of *p53* frequently accompany the depletion of p53 activation and a reduction of tumor cell apoptosis. However, mutations do not inevitably lead to the inhibition of apoptosis. UVB could indeed trigger apoptosis in *p53*-mutated or -depleted epithelioid cells[4,5,8].

Cells undergoing apoptosis display a number of characteristic biochemical and morphological changes, such as chromatin condensation, DNA cleavage, loss of mitochondrial membrane potential ($\Delta\Psi m$) and cell shrinkage. The sequence of such apoptotic events varies significantly from one cell type to another depending on the cell type as well as apoptotic stimuli[8–11]. For a long time, DNA has been regarded as the only molecular cellular target for UVB and UVC. However, evidence is accumulating that UV can also affect cytoplasmic and membrane structures[12].

The activation of caspases plays a pivotal role in the execution phases of apoptosis. Recent advances in caspase research have greatly enhanced our knowledge concerning the implications of caspase cascades in apoptosis induced by various stimuli[13,14]. Caspases are normally present in cells as proenzymes that require limited proteolysis for the activation of enzymatic activity. They are currently divided into two classes: activator and effector. The former includes caspase–8, –9 and –10, whereas the latter includes caspase–3, –6 and –7. Activator caspases propagate the apoptotic signal by the proteolytic activation of effector caspases. The activation of several caspases occurs sequentially. Such sequential activation events are, therefore, called a caspase cascade. The activated effector caspases then execute the final cell death program through the degradation of vital proteins. Studies on the molecular regulation of caspase activation have revealed that mitochondria and mitochondrion-derived factors are responsible for coordinating the events[15,16].

Two main caspase cascades have been delineated in mammalian cells. The first one links caspase-8 to death receptors, such as Fas and TNFR1, expressed at the cell surface. Several observations have suggested a role of Fas/FasL and TNFR in the pathways in response to DNA damage in various cells[17–20]. In the second pathway, procaspase–9 is activated by a wide variety of death stimuli, including DNA damaging agents. The release of cytochrome *c* from mitochondria plays a crucial role in the activation[15]. Both active caspase–8 and caspase–9 can cleave and activate an overlapping set of effector caspases, including caspase–3, –6 and –7.

A panel of peptide inhibitors, specific for each caspase, has been utilized for investigating the involvement of caspase(s) in particular apoptotic processes[1,5,8,10,11,21]. Iwasaki et al reported the rapid development of apoptosis in *p53*-mutated A431 cells following UVB exposure and the inhibition of apoptosis by caspase–1 and –3 inhibitors[5]. For UVC-induced apoptosis, however, the involvement of individual activator and/or effector caspases and their

exact order within the apoptotic cascade remains obscure.

In the present study, we investigated the sequential order of apoptotic events, such as chromatin condensation, $\Delta\Psi m$ and dye uptake, in UVC-irradiated A431 cells. In addition, we explored the cell-cycle dependency of apoptosis and the effects of specific caspase inhibitors in order to define the caspase cascade specific to UVC-induced apoptosis in A431 cells.

MATERIALS AND METHODS

Reagents

All biochemicals were purchased from Sigma chemicals unless otherwise specified. Hoechst 33342 was dissolved in distilled water to give a final concentration of 1.0 μM. 3,3' dihexyloxacarbocyanine iodide ($DiOC_6(3)$) was purchased from Molecular Probes, Inc., (Eugene, OR, USA). Caspase inhibitors were obtained from Peptide Institute Inc. (Osaka, Japan) and dissolved in DMSO.

Cell culture

An A431 cell line was obtained from Health Science Research Resources (Osaka, Japan). A431 cells bear a mutated *p53* gene. Cells were grown in Dulbecco's modified Eagle's medium (Nissui Seiyaku, Tokyo, Japan) supplemented with 10% fetal bovine serum (CSL, Australia) inactivated at 55°C, 30 min, 4 mM L-glutamine, glucose (4.5 g/L), $NaHCO_3$, 50 units/ml penicillin and 50 μg/ml streptomycin (Gibco-BRL, USA) in a humidified atmosphere containing 5% CO_2 at 37°C.

The cells were seeded at 2×10^5 cells per dish in a 60 mm-culture dish in the growth medium and subcultured when grown to 80% confluence using 0.25% trypsin (Gibco-BRL, USA). When grown to 50% confluence, cells were treated with different doses of UVC radiation. Inhibitors of caspases were added to the incubation medium 2 h before UVC-irradiation to give a final concentration of 100 μM.

UVC-irradiation and dosimetry

A UV light source was a germicidal lamp (Model UVG-54, Ultra-Violet Products), emitting UVC with the peak at 254 nm. The fluence rate was 0.5 W/m^2, as determined by a UV digital radiometer (Model UVX Digital Radiometer, Ultra-Violet Products) with a Model UVX-25 sensor[22]. Irradiation was performed at least 2 h after seeding when cells were well attached. The DMEM was removed and cells were washed once with PBS (–) before irradiation with various doses of UVC ranging from 0 to 50 J/m^2.

Determination of apoptotic chromatin condensation

Apoptotic chromatin condensation induced by UVC was identified and quantitated by fluorescent microscopy after being stained with Hoechst 33342, as previously described[23]. The number of cells with chromatin condensation was scored as apoptotic cells. Three or more randomly selected areas were observed for each sample, and 200 or more cells were

examined to determine the fraction of cells with chromatin condensation.

Flow cytometric analysis —Analysis of Sub G_1 population and cell cycle phases

Apoptotic cells with DNA fragmentation were determined by flow cytometry after the extraction of DNA fragments according to a method of Cock et al[24] using a flow cytometer, Epics XL (Couler, Hialeah, Fa). After being lysed in 0.1% sodium citrate and 0.1% Triton X-100, and stained with propidium iodide (PI: 50 μg/ml), cells with DNA fragmentation were identified as a sub-G_1 fraction of cells with lower DNA content. A cell-cycle phase analysis was performed using a ModFit program (Becton Dickinson, San Jose, CA, USA).

Flow cytometric analysis—Mitochondrial transmembrane potential ($\Delta\Psi$m) and dye uptake

The $\Delta\Psi$m was evaluated by staining cells with ($DiOC_6$ (3)), a fluorochrome incorporated into cells dependent on their $\Delta\Psi$m, according to the method described by Zamzami et al[25]. Briefly, after being stained for 10 min at 37°C with 40 nM of $DiOC_6$(3), the cells were subsequently stained with PI (10 μg/ml PBS) to evaluate dye uptake (plasma membrane integrity). Live or early apoptotic cells exclude PI, while necrotic or late apoptotic cells were stained with PI. The analysis was performed by flow cytometry using an Epics XL. Fl-1 and Fl-4 emissions were detected for $DiOC_6$(3) and PI staining, respectively. The cell population with distinctly lower FSC and higher SSC was judged as shrunken cells.

RESULTS

Time- and dose-dependent induction of apoptosis in A431 cells following UVC exposure

The number of cells detached from the dish increased with increasing UV dose and time

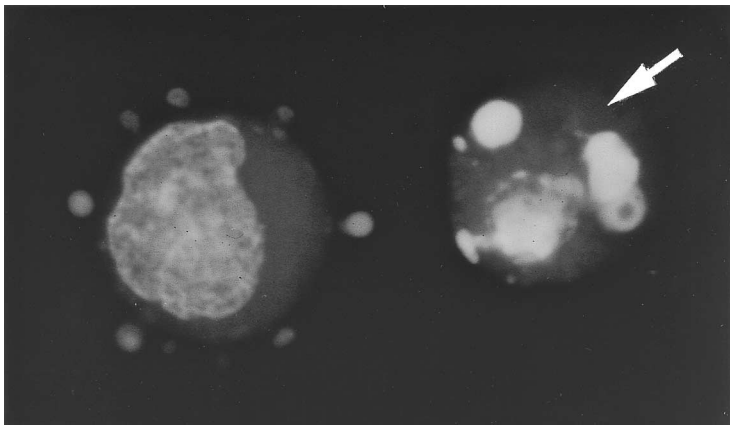

Fig. 1. Apoptotic A431 cells visualized with a fluorescent microscope after being stained by DNA-binding fluorophor Hoechst 33342. The morphological characteristics of apoptosis, such as chromatin condensation and nuclear fragmentation (indicated by arrow), distinctly different from a normal cell (left), are clearly seen.

after exposure to UVC. The detached cells showed morphological changes characteristic of apoptosis (chromatin condensation, blebbing, and nuclear fragmentation) under a fluorescent microscopic observation after staining with DNA-binding fluorophor Hoechst 33342 (Fig. 1). Most of chromatin condensed cells showed nuclear fragmentation and were clearly distinguished from normal viable cells. Cells with chromatin condensation began to increase 2 h after 20 J/m^2 UVC irradiation from about 0% to approximately 60% at 8 h and reached nearly 80% by 24 h (Fig. 2A). The dose-dependent increase in apoptotic cells 12 h after UVC is

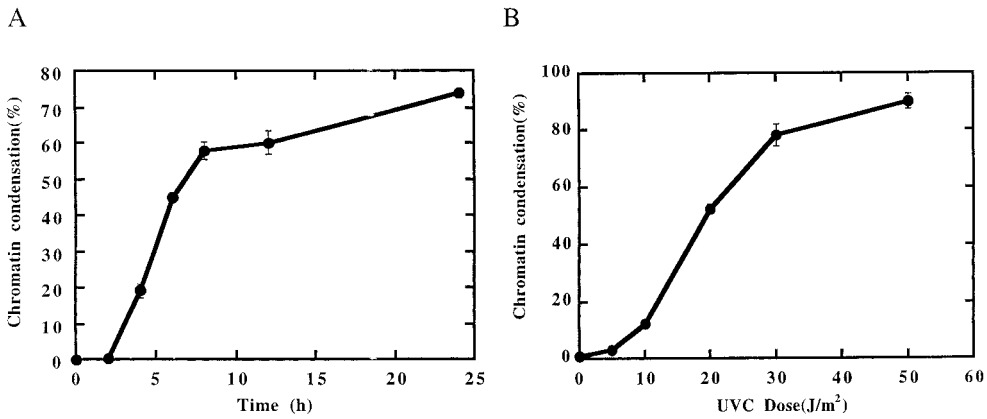

Fig. 2. Time and dose dependent appearance of apoptotic A431 cells (defined by chromatin condensation) after exposure to UVC. (A) Time-course for the induction of apoptosis after 20 J/m^2 UVC irradiation. The percentage of chromatin condensed cells is plotted against time (h) after irradiation. (B) Dose-response curve for UVC-induced apoptosis. Apoptotic cells were counted 12 h after UVC irradiation with the doses given on the abscissa. The bars represent mean ± S.E.M.

shown in Fig. 2B. Apoptotic cells gradually rose from 10% at 10 J/m^2 to 80% at 30 J/m^2, and more than 90% of the cells underwent apoptosis by 50 J/m^2 UVC. These results clearly indicate that apoptosis in A431 cells appears within 12 h after UVC irradiation.

Based on the present findings, together with the fact that the doubling time of A431 cells was approximately 12 h, we concluded that the UVC-induced apoptosis in A431 occurred within one cell cycle before mitosis and was, therefore, mainly of the interphase death type.

Increase in sub-G_1 cells after UVC-exposure independent of cell cycle phases

Several lines of evidence indicate that the intrinsic sensitivity of cells to DNA damaging agents is a function of the position in the cell cycle. The effects of UVC exposure on cell-cycle progression and apoptotic DNA fragmentation in A431 were analyzed by flow cytometry. As shown in Fig. 3, cells with "sub-G_1" DNA content, representing cells with DNA fragmentation accumulated gradually from 4 h after 20 J/m^2 irradiation and reached about 50 % at 12 h, almost in parallel with an increase in apoptotic cells having chromatin condensation. During the course of the 12-h incubation after UVC-exposure, the percentages of G_1-, S- and G_2/M-phase cells changed only slightly. These results suggest that the UVC

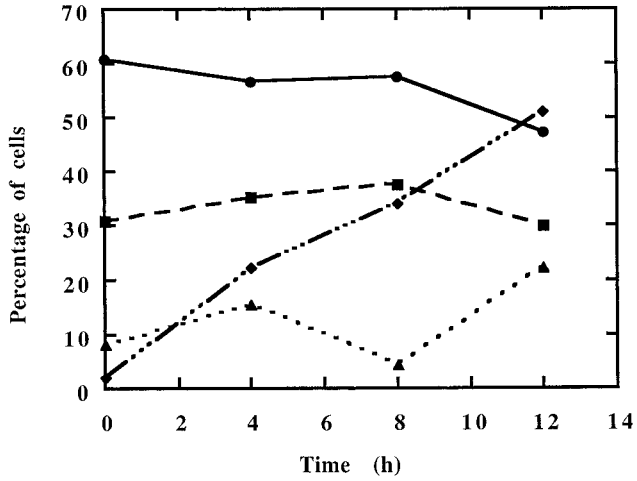

Fig. 3. Changes in the cellular distribution among the cell cycle phases with time after 20 J/m^2 UVC irradiation. The closed diamonds with a solid-dotted mixed line represent the sub-G_1 (apoptotic) fraction; the closed circles with a solid line, the G_1 fraction; the closed squares with a broken line, the S fraction; the closed triangles with a dotted line, the G_2/M fraction.

sensitivity of A431 cells does not vary substantially as a function of the cell-cycle phase, provided that asynchronized cells are used.

Early loss in ΔΨm precedes cell shrinkage and dye uptake in UVC-induced apoptosis

Recent studies have suggested that mitochondria are involved in initiating the active phase of apoptosis[15,16]. A decrease in the mitochondrial transmembrane potential, ΔΨm, is reported to function as an early signal for apoptosis in most kinds of apoptosis[26]. The relationship between the onset of ΔΨm loss and UV-induced apoptosis progression is not fully clarified. It is, therefore, of interest to measure ΔΨm in parallel with other cell death markers during the course of apoptosis. Simultaneously, we measured PI staining to identify cell death with loss of structural integrity of the plasma membrane. Representative dot plots of $DiOC_6(3)$- and PI-staining are shown in Fig. 4A. Double staining of cells with $DiOC_6(3)$ and PI made it possible to relate changes in the plasma membrane potential to a distinct stage of apoptosis. Control cells were comprised of highly $DiOC_6(3)$-stained and low PI-stained cells, reflecting the intact mitochondrial membrane potential and plasma membrane permeability. In contrast, 12 h after exposure, about 80% of the cells showed discretely lower $DiOC_6(3)$ staining, and 50% of the cells had distinctly higher PI staining. An analysis of the forward scatter (FSC) and side scatter (SSC) dot plot revealed the existence of a discretely lower FSC and higher SSC population, namely, a shrunken cell- or apoptotic body-population, in the irradiated cell population (Fig. 4A).

Figure 4B shows time-dependent changes in PI high, ΔΨm low and shrunken cells after exposure to 20 J/m^2 UVC. The cells with reduced ΔΨm emerged as early as 2 h and increased progressively with time, reaching to 80% by 12 h. Therefore, impairment of ΔΨm is the first

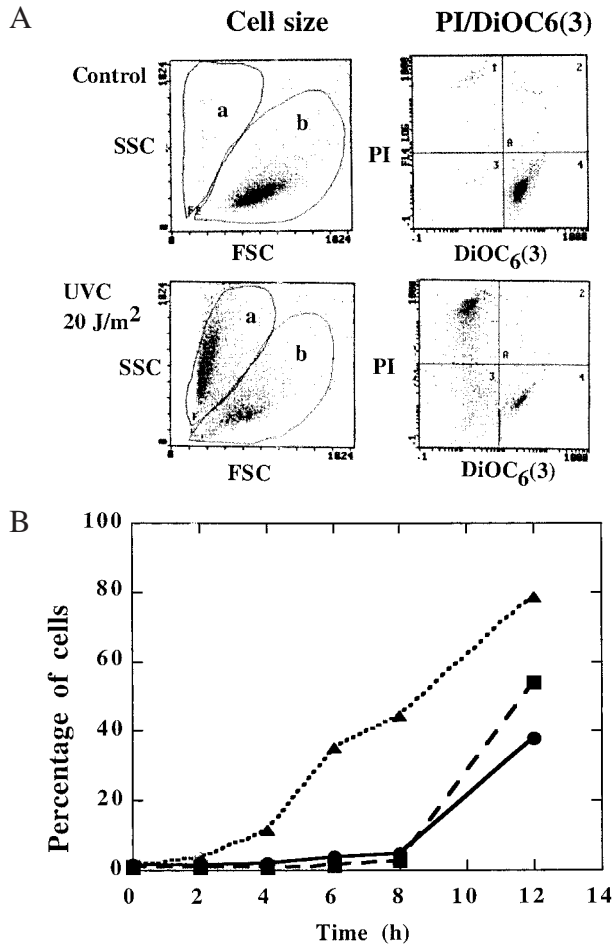

Fig. 4. Flow cytometric analysis of apoptotic changes in A431 cells following exposure to 20 J/m^2 UVC. (A) Representative dot plots for a dual staining ($DiOC_6(3)$ and PI) experiment with flow cytometry. The analysis was performed using Coulter Epics XL after staining with $DiOC_6(3)$ (for $\Delta\Psi$m assay) and PI (for dye exclusion test). The left panels represent dot plots in which the side scatter intensities (SSC) are plotted against the forward scatter ones (FSC). The upper-left panel shows data for non-irradiated control cells, and the lower-left one, for the cells 12 h after 20 J/m^2 UVC irradiation. The cell population with distinctly lower FSC and higher SSC was judged as shrunken cells (detected in region a). The right panels represent dot plots in which the Fl-1 (PI) emission intensities are plotted against the Fl-4 ($DiOC_6(3)$) ones. The upper-right panel represents the data for non-irradiated control cells and the lower-right panel, the data for the cells 12 h after 20 J/m^2 UVC irradiation. Live or early apoptotic cells exclude PI, while necrotic or late apoptotic cells were stained with PI.

(B) Time-course for the percentage of cells showing low $\Delta\Psi$m, high PI emission or small size, which are represented by the closed triangles with a dotted line, the closed squares with a broken line and the closed circles with a solid line respectively. The irradiated cells were sampled at various times given on the abscissa after irradiation for the analysis by flow cytometry, as shown in the Text and in Fig. 4 (A).

identifiable change at the onset of the UVC-induced apoptosis in A431 cells. The chromatin condensation and DNA fragmentation mentioned above appeared later, at around 4 h. Measurements of the alterations of $\Delta\Psi m$ and the plasma membrane permeability by simultaneous dual-color staining revealed that cells with reduced fluorescence $DiOC_6(3)$ concomitantly admitted an increasing amount of PI. The impairment of membrane permeability (PI staining) and cell shrinkage, detected as lower FSC and higher SSC populations, appeared almost simultaneously in the late stage of apoptosis, at around 8 h. Dose-dependent increases in $DiOC_6(3)$ low, PI high and shrunken cells were observed (data not shown).

These results clearly indicate the sequence of events within the UV-induced apoptosis in A431 cells. It begins with the reduction of $\Delta\Psi m$ during the earliest phase, followed by the appearance of chromatin condensation and DNA fragmentation, and the final precipitous cell death with the impairment of integrity in membrane permeability and cell shrinkage.

Inhibition of UVC-induced apoptotic changes by caspase inhibitors

To clarify the caspase cascade involved in UVC-induced apoptosis in A431, we examined the effect of 6 caspase inhibitors on the apoptotic events mentioned above. As shown in Fig. 5, the incubation of A431 cells with z-VAD-fmk, a peptide caspase inhibitor with broad specificity, almost completely inhibited all of the characteristic apoptotic changes, except for $\Delta\Psi m$. A caspase–1 inhibitor, Ac-YVAD-CHO, had no preventive effect. A caspase–3/7 inhibitor, Ac-DEVD-CHO, considerably inhibited apoptosis, but was less effective compared with z-VAD-fmk.

These data suggest that caspase(s) other than caspase-1 is involved in apoptosis. Therefore, we further examined 2 inhibitors of activator caspases, namely, Ac-IETD-CHO, a

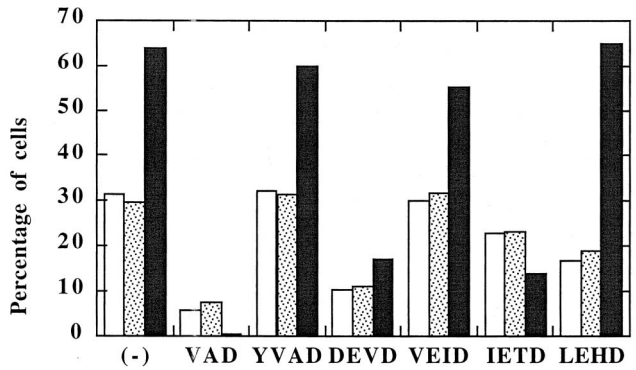

Fig. 5. Effect of the caspase inhibitors on UVC-induced apoptosis in A431. Cells were preincubated 2 h with 100 μM inhibitors prior to 20 J/m^2 UVC-exposure to ensure penetration of inhibitors into cells. At 12 h after irradiation, the percentage of cells showing shrinkage (open columns), PI-stained cells (dotted columns), or chromatin condensation (closed columns) were measured by flow cytometry, as described in the Legend for Fig. 4A, with or without 5 caspase inhibitors, the abbreviated names of which are given on the abscissa. VAD, z-VAD-fmk; YVAD, Ac-YVAD-CHO; DEVD, Ac-DEVD-CHO; VIED, Ac-VIED-CHO; IETD, Ac-IETD-CHO; LEHD, Ac-LEHD-CHO.

caspase–8/6 inhibitor, and Ac-LEHD-CHO, a caspase–9 inhibitor. The former inhibited chromatin condensation effectively almost comparable to the inhibitor of caspase-3. However, it only partially inhibited the cell death detected by PI staining and cell shrinkage. Although both inhibitors suppressed PI staining and cell shrinkage, almost to the same extent, the caspase–9 inhibitor could not prevent chromatin condensation. Because Ac-IETD-CHO was also known to inhibit caspase-6, we further examined the effect of a specific inhibitor of caspase–6 (Ac-VEID-CHO) to clarify whether or not caspase-6 participated in the apoptotic process. As shown in Fig. 5, the inhibitor of caspase–6 did not prevent all of the apoptotic changes. Therefore, the possibility of the involvement of caspase–6 in the apoptotic processes could be excluded.

These data demonstrate an important role of capsase–3/7 and caspase–8 cascade for UVC-induced apoptosis in A431 cells. Furthermore, the data suggest that caspase–9 cascade seems to be less important, though it may contribute to some extent.

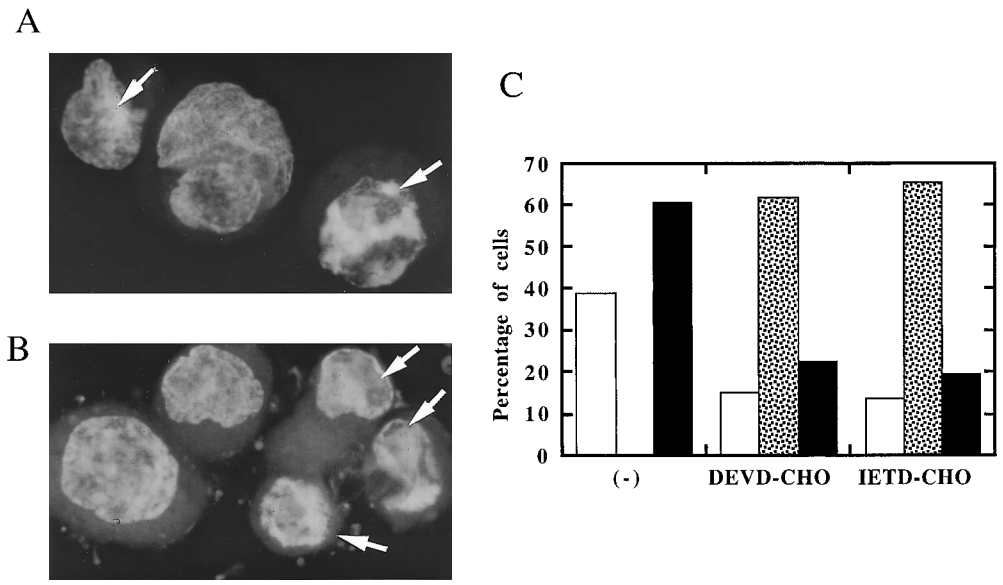

Fig. 6. Effect of Ac-DEVD-CHO, a caspase-3/7 inhibitor and Ac-IETD-CHO, a caspase–8 inhibitor, on chromatin condensation of UVC-irradiated A431 cells. Cells having the intermediate-type chromatin condensation (indicated by arrow) after a treatment with a caspase –3/7 inhibitor, Ac-DEVD-CHO (A), and a caspase–8 inhibitor, Ac-IETD-CHO (B). A431 cells were treated with the inhibitor and irradiated with UVC, as described in the Legend for Fig. 5. Chromatin condensation was visualized with a fluorescent microscope after being stained by Hoechst 33342 12 h after UVC irradiation. (C) Percentages of cells having normal (open columns), intermediate-type chromatin condensation (dotted columns) and typical apoptotic chromatin condensation (closed columns) were estimated after treatments with the inhibitors described on the abscissa under the conditions described in the Legends for Figs. 6A and 6B. (–) represents the data for the cells without any treatment of the inhibitors, but were incubated for 12 h after the UVC irradiation; DEVD-CHO, for the cells treated with a caspase-3/7 inhibitor, Ac-DEVD-CHO; IETD-CHO, for the cells treated with a caspase-8 inhibitor, Ac-IETD-CHO.

We described above that caspase–3/7 and –8/6 inhibitors inhibited chromatin condensation. A careful observation revealed, however, that the chromatin in the exposed cells exhibited the intermediate-type chromatin condensation without nuclear fragmentation after a treatment with the caspase–3 or –8 inhibitor (Figs. 6A and 6B). The intermediate-type condensation can be easily distinguished from typical chromatin condensation by the absence of nuclear fragmentation, although distinction between the normal and intermediate type was difficult. A preliminary observation using an arbitrary classification for the condensation types revealed that most of the potentially apoptotic nuclear condensation was partially inhibited by caspase–3 and –8 inhibitors (Fig. 6C). On the other hand, chromatin condensation was completely prevented by a treatment with pan-caspase inhibitor, z-VAD-fmk. Taken together, the data suggest that, in addition to caspase–3/7 or –8/6, other caspase(s) might be involved in the typical chromatin condensation with nuclear fragmentation.

None of these five inhibitors could completely prevent the UVC-induced impairment of $\Delta\Psi$m. z-VAD-fmk, however, inhibited the depletion of $\Delta\Psi$m, partially to an intermediate level, as shown in Fig. 7A. Figure 7B shows that the percentages of cells having low and intermediate $\Delta\Psi$m did not decrease after the treatment of caspase inhibitors. These data suggest that, even though reduction in $\Delta\Psi$m occurred at an earlier stage following UVC-exposure, it

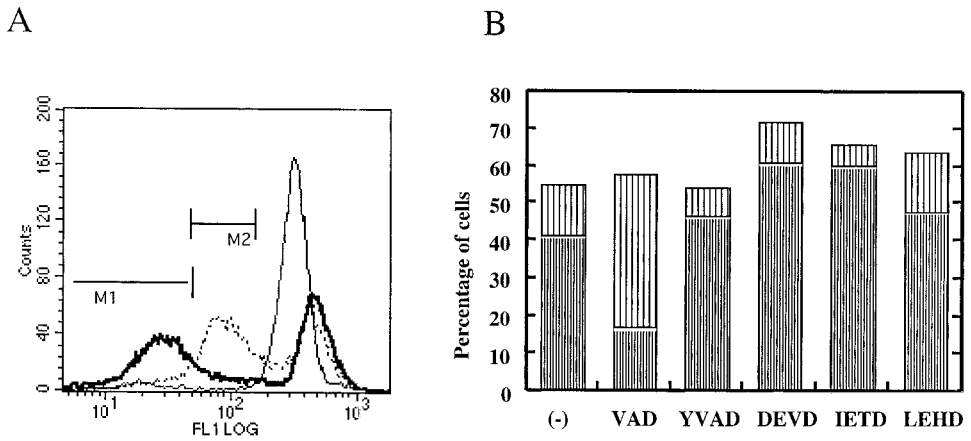

Fig. 7. Effect of caspase inhibitors on the distribution of cells having intermediate or low $\Delta\Psi$m. (A) Representative histograms of distribution of cells having high, intermediate and low fluorescence intensities of $DiOC_6(3)$. The loss of mitochondrial transmembrane potential, $\Delta\Psi$m, in A431 cells after 20 J/m^2 UVC irradiation was measured with flow cytometry as shown in the Text and in Fig. 4A, to estimate the percentage of cells showing high (reprensented by the right 2 peaks), intermediate (shown by the range bar M2) and low (M1) $\Delta\Psi$m. The histograms represent non-irradiated control (shown by thin line), 20 J/m^2 UVC irradiated (solid line) and z-VAD-treated + UVC irradiated (dotted line) cells, respectively.

(B) Effect of caspase inhibitors on the distribution of cells having intermediate or low $\Delta\Psi$m. The distributions of $\Delta\Psi$m were measured as described in the Legend for Fig. 7A. The percentages of cells having intermediate $\Delta\Psi$m are represented by sparsely striated columns; the percentages of cells having low $\Delta\Psi$m, densely striated columns. (–), data for the cells without any inhibitor; other data for the cells treated with 5 caspase inhibitors, abbreviated names of which are given on the abscissa. VAD, z-VAD-fmk; YVAD, Ac-YVAD-CHO; DEVD, Ac-DEVD-CHO; IETD, Ac-IETD-CHO; LEHD, Ac-LEHD-CHO.

may not play a central role for the development of apoptotic cell death in A431 cells.

Ineffectiveness of the protectors of ΔΨm reduction

To substantiate our finding that apoptosis can proceed without a decrease in ΔΨm, we examined effect of cyclosporin A and bongkrekic acid on apoptosis. It has been postulated that cyclosporin A inhibits the mitochondrial megachannel, which is also called the permeability transition (PT) pore, and that bongkrekic acid inhibits the disruption of ΔΨm and apoptosis through the action on another putative constituent of megachannel, adenine nucleotide translocator[16]. Opening of the pore has dramatic consequences on the mitochondrial physiology, including ΔΨm. As shown in Fig. 8, cyclosporine A at concentrations from 1 to 50 μM (data not shown) could not inhibit apoptotic chromatin condensation. It also did not inhibit the reduction of ΔΨm (data not shown). The addition of bongkrekic acid had no preventive effect on the induction of apoptotic chromatin condensation in cells exposed to 20 J/m^2 (Fig. 8).

These results support the dispensability of the disruption of ΔΨm for UVC induced apoptosis.

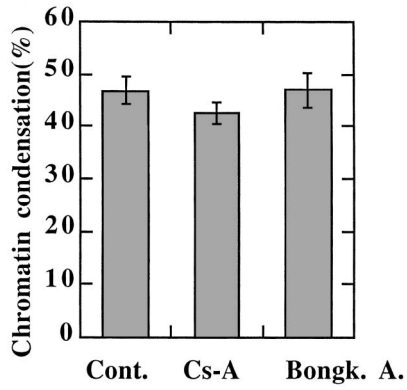

Fig. 8. Effect of cyclosporine A and bongkrekic acid on the UVC-induced apoptosis in A431 cells. The percentage of cells with chromatin condensation was measured 12 h after UVC irradiation without the addition of a reagent (shown as Cont.), with the treatment with 10 μM cyclosporine A (Cs-A) or with 25 μM bongkrekic acid (Bongk. A.).

DISCUSSION

The results of our present study showed sequential characteristic changes of apoptosis in *p53*-mutated A431 cells after UVC exposure and the involvement of caspases for the apoptotic processes.

UVC-induced apoptosis is independent of the cell cycle phases

DNA-damaging agents including UVB and UVC are known to stabilize the p53 protein,

which then functions as a cell-cycle checkpoint by leading to growth arrest or apoptosis[6]. The present study using *p53*-mutated A431 cells revealed that only a minor change in the cell-cycle phase took place after UVC-exposure. A similar independence of UVC-induced apoptosis from the cell cycle was reported for OCP13, a Medaka cell line[3]. Wang et al reported that UVC, unlike X-rays, caused the down-regulation of a cell-cycle inhibitor, p21, in human cancer cells independently of p53[27]. They also observed significant dose-dependent changes in the cell-cycle kinetics in UVC-treated mutant *p53* cells, despite a decrease in p21. Inconsistent with this result, p21 expression in fibroblast cell lines was transcriptionally activated by UVC in a p53-independent manner[28]. Thus, the mechanisms of apoptosis must vary depending on cell lines different from each other in *p53* mutation.

Roles of mitochondrial disfunction

The activation of apoptotic execution is suggested to be associated with the loss of mitochondrial transmembrane potential resulting from the formation of a permeability transition (PT) pore. Cytochrome *c* and procaspases–3, –9 etc. have been shown to release from mitochondria prior to apoptotic execution[16]. $\Delta\Psi$m has been known to be one of the earliest universal changes in apoptosis. This has led to the proposal that mitochondrial depolarization represents a central irreversible checkpoint in the apoptotic program. Recent data suggest, however, that the collapse of $\Delta\Psi$m is not always an early marker for apoptosis[9]. It occurs in the late phase, and is not a part of the central apoptotic machinery in HL60[29]. In the present study, depletion of $\Delta\Psi$m indeed appeared during the earliest phase of apoptosis in UVC-induced apoptosis in A431. Experiments using caspase inhibitors (Figs. 5, 6 and 8) suggest, however, that $\Delta\Psi$m disruption is dispensable for the central apoptotic machinery. This is further supported by the findings that 2 inhibitors (cyclosporine A and bongkrekic acid) known to protect of mitochondrial $\Delta\Psi$m could not protect against apoptosis (Fig. 8). Dose- and time-dependent depletion of $\Delta\Psi$m took place in Jurkat T cells after UVA1 (340–400 nm) exposure[2]. Cyclosporine A prevented UVA1-triggered immediate apoptosis, but did not block the immediate depolarization of micochondrial membranes. In transformed lymphocytes, UVA1 radiation primarily mediates singlet-oxygen damage triggering immediate apoptosis ($T < 20$ min) by immediately opening the cyclosporine A-sensitive mitochondrial megapore, while superoxide anions initiate another cyclosporine A-insensitive final apoptotic pathway[30]. Thus, the extent of the involvement of mitochondrial change in apoptosis considerably varies depending on the triggers of apoptosis as well as on the cell lines.

Involvement of caspase cascade

Iwasaki et al reported the involvement of caspase–1 and –3 in UVB induced apoptosis in A431 cells. The sequential activation of caspase–8, –3 and –1 also in UVB[8] and in radiation-induced apoptosis has been reported. In the present study we examined 6 caspase inhibitors on 5 apoptotic changes (Fig. 5). The results confirmed a pivotal role of caspases and clearly demonstrated that a caspase cascade involving caspases–8 and –3 is the main pathway working in UVC-induced apoptosis in A431.

It is of interest to note that the caspase–8 inhibitor suppressed chromatin condensation to

almost comparable extent with that shown by the caspase–3 inhibitor, though it inhibited PI-staining and cell shrinkage only partially. The results indicate that caspase–8 plays at least some roles as an upstream activator caspase. The possibility remained that caspase–8/6 inhibitor, Ac-IETD-CHO, exerted its effect through the inhibition of caspase–6. This was denied, however, by an experiment using caspase–6 inhibitor (Ac-VEID-CHO) (Fig. 5).

The direct activation of Fas, an upstream component of the caspase–8 cascade, was shown to mediate UV-induced apoptosis in the human keratinocyte cell line: HaCaT, MCF7 and BJAB[18,31]. It was also reported that DNA damaging agents including UV induce the expression of the Fas ligand and subsequent apoptosis in T lymphocytes via the activation of NF-κB and AP-1[32]. UV was also known to stimulate the aggregation-mediated activation of TNFR1, which was coupled with an activation of caspase–8, although another genotoxic agent, such as ionizing radiation, cisplatin and melphalaan, induced apoptosis without TNFR aggregation. These findings suggest that the signaling for UV-induced apoptosis was different from those for apoptosis induced by other agents, and that UV induced the direct aggregation of the TNFR receptor[20]. The involvement of Fas expression and TNF in the activation of caspase–8 in A431 is now under investigation.

The role of the caspase–9 cascade in the apoptosis in A431 remains to be examined. The inhibitor of caspase–9 partially suppressed cell shrinkage and cell death to almost a comparable extent to that induced by the caspase–8 inhibitor. Unlike the caspase-8 inhibitor, however, it could not inhibit chromatin condensation. Cytochrome *c*, an essential component for caspase–9 activation, must be released from mitochondria. Bossy-Wetzel et al observed that cytochrome *c* released from mitochondria independently of mitochondrial transmembrane depolarization in T lymphoblastoid cell line, CEM, after exposure to UVB[33]. Moreover, they also reported that a caspase inhibitor, z-VAD-fmk, effectively blocked the reduction in $\Delta\Psi m$, but failed to block the release of cytochrome *c*. Cytochrome *c* passed through the outer mitochondrial membrane in the earlier phase after X-ray irradiation and $\Delta\Psi m$ reduction in cellular and isolated mitochondria occurred during a late phase after a considerable loss of cytochrome *c*[32].

In addition to the caspase–8 and –3/7 cascade, which can be partly involved in the mechanism underlying the UVC-induced apoptosis in A431, other unknown caspase cascade(s) must operate, since the caspase-8 inhibitor could only partially inhibited apoptotic events, while a pan caspase inhibitor, z-VAD-fmk, almost completely inhibited these events. Further studies are needed to clarify the caspase cascades completely.

Roles of caspases in the execution phase

Hirata et al suggested that caspase–6 and –3 play major roles in nuclear apoptosis[21]. Caspase–6 cleaves nuclear mitotic apparatus protein (nuclear matrix protein) and mediates the shrinkage and fragmentation of nuclei. Caspase–3 cleaves nuclear matrix protein at sites different from those cleaved by caspase–6 and mediate DNA fragmentation and chromatin condensation. Caspase(s) distinct from caspase–3 or –6 mediates the disruption of the mitochondrial membrane potential and the shrinkage of cytoplasm.

Chromatin condensation was completely prevented by a treatment with a pan-caspase inhibitor, z-VAD-fmk, but most of the potentially apoptotic nuclear condensation was par-

tially inhibited by caspase–3 and –8 inhibitors (Fig. 6C). These findings strongly suggest the participation of additional caspase(s), other than caspase–3, for complete chromatin condensation. Recently, Sahara et al found Acinus, a new nuclear factor, which induced apoptotic chromatin condensation after cleavage by caspase–3[34]. They propose that additional protease(s) are required for full activation. Several factors, such as caspase activated DNase (CAD) and apoptosis inducing factor (AIF) etc., have indeed been reported to induce chromatin condensation[35].

Hakem et al observed that embryonic stem cells and embryonic fibroblast cells from caspase–9 knockout mice were resistant to several apoptotic stimuli including UV and γ-radiation, while thymocytes were sensitive to UVC, but not to γ-rays[36]. Therefore, caspase-9 is required for γ-ray- but not for UV-induced apoptosis in thymocytes. Partial dependency of UVC-induced apoptosis in A431 cells on caspase-9 reported here (Fig. 5) suggests its similarity to UV-induced apoptosis in thymocytes.

ACKNOWLEDGEMENTS

This work was supported in part by a Special Grant for Promoted Research from National Institute of Radiological Sciences.

REFERENCES

1. Kimura, C., Zhao, Q. L., Kondo, T., Amatsu, M. and Fujiwara, Y. (1998) Mechanism of UV-induced apoptosis in human leukemia cells: roles of Ca^{2+}/Mg^{2+}-dependent endonuclease, caspase–3, and stress-activated protein kinases. Exp. Cell Res. **239**: 411–422.
2. Goder, D. E. and Lucas, A. D. (1995) Spectral dependence of UV-induced immediate and delayed apoptosis: the role of membrane and DNA damage. Photochem. Photobiol. **62**: 108–113.
3. Nishigaki, R., Mitani, H. and Shima, A. (1998) Evasion of UVC-induced apoptosis by photorepair of cyclobutane pyrimidine dimers. Exp. Cell Res. **244**: 43–53.
4. Gniadecki, R., Hanson, M. and Wulf, H. C. (1997) Two pathways for induction of apoptosis by ultraviolet radiation in cultured human keratinocytes. J. Invest. Dermatol. **109**: 163–169.
5. Iwasaki, K., Izawa, M. and Mihara, M. (1997) Involvement of caspases in apoptosis induced by ultraviolet B irradiation in A431 human epithelioid tumor cells. Biochem. Mol. Biol. Int. **42**: 1271–1279.
6. Burns, T. F. and El-Deiry, W. S. (1999) The p53 pathway and apoptosis. J. Cell. Physiol. **181**: 231–239.
7. Ghosh, J. C., Suzuki, K., Kodama, S. and Watanabe, M. (1999) Effects of protein kinase inhibitors on the accumulation kinetics of p53 protein in normal human embryo cells following X-irradiation. J. Radiat. Res. **40**: 23–37.
8. Takahashi, H., Nakamura, S., Asano, K., Kinouchi, M., Ishida-Yamamoto, A. and Iizuka, H. (1999) Fas antigen modulates ultraviolet B-induced apoptosis of SVHK cells: sequential activation of caspases 8, 3, and 1 in the apoptotic process. Exp. Cell Res. **249**: 291–298.
9. Ferlini, C., Angelis, C. D., Biselli, R., Distefano, M., Scambia, G. and Fattorossi, A . (1999) Sequence of metabolic changes during X-ray-induced apoptosis. Exp. Cell Res. **247**: 160–167.
10. Rokhilin, O. W., Glover, R. A. and Cohen, M. B. (1998) Fas mediated apoptosis in human prostatic carcinoma cell lines occurs via activation of caspase-8 and caspase-7. Cancer Res. **58**: 5870–5875.

11. Tepper, A., de Vries, E., van Blitterswijk, W. J. and Borst, J. (1999) Ordering of ceramide formation, caspase activation, and mitochondrial changes during CD95- and DNA damage-induced apoptosis. J. Clin. Invest. **103**: 971–978.
12. Schwarz, T. (1998) UV light affects cell membrane and cytoplasmic targets. J. Photochem. Photobiol. B: Biol. **44**: 91–96.
13. Nuñet, G., Benedict, M. A., Hu, Y. and Inohara, N. (1998) Caspases: the proteases of the apoptotic pathway. Oncogene **17**: 3237–3245.
14. Green, D. R. (1998) Apoptotic pathways: the road to ruin. Cell **94**: 695–698.
15. Mignotte, B. and Vayssiere, J.-L. (1998) Mitochondria and apoptosis. Eur. J. Biochem. **252**: 1–15.
16. Kroemer, G., Dallaporta, B. and Resche-Rigon, M. (1998) The mitochondrial death /life regulator in apoptosis and necrosis. Ann. Rev. Physiol. **60**: 619–642.
17. Caricchio, R., Reap, E. A. and Cohen, P. L. (1998) Fas/Fas ligand interactions are involved in ultraviolet-B-induced human lymphocyte apoptosis. J. Immunol. **161**: 241–251.
18. Aragane, Y., Kulms, D., Metze, D., Wilkes, G., Poppelmann, B., Luger, T. A., and Schwarz, T. (1998) Ultraviolet light induces apoptosis via direct activation of CD95(Fas/APO-1) independently of its ligand CD95L. J. Cell Biol. **140**: 171–182.
19. Leverkus, M., Yaar, M. and Gilchrest, B. (1997) Fas/Fas ligand interacton contributes to UV-induced apoptosis in human keratinocytes. Exp. Cell Res. **232**: 255–262.
20. Sheikh, M. S., Antinore, M. J., Huang, Y. and Fornace Jr., A. J. (1998) Ultraviolet-irradiation-induced apoptosis is mediated via ligand independent activation of tumor necrosis factor receptor 1. Oncogene **17**: 2555–2563.
21. Hirata, H., Takahashi, A., Kobayashi, S., Sawai, H., Okazaki, T., Yamamoto, K. and Sasada, M. (1998) Caspases are activated in a branched protease cascade and control distinct downstream processes in Fas-induced apoptosis. J. Exp. Med. **187**: 587–600.
22. Wang, B., Fujita, K., Watanabe, K., Mitani, H., Yamada, T. and Shima, A. (1997) Induction of apoptosis in cultured midbrain cells from embryonic mice. Radiat. Res. **147**: 304–308.
23. Hama-Inaba, H., Wang, B., Mori, M., Matsushima, T., Saitoh, T., Takusagawa, M., Yamada, T., Muto, M. and Ohyama, H. (1998) Radio-sensitive murine thymoma cell line 3SB: characterization of its apoptosis-resistant variants induced by repeated X-irradiation. Mutat. Res. **403**: 85–94.
24. Boesen-de Cock, J. G. R. , Tepper, A. D., de Vries, E., Blitterswijk, W. J. and Borst, J. (1999) Common regulation of apoptosis signaling induced by CD95 and the DNA-damaging stimuli etoposide and γ-radiation downstream from caspase-8 activation. J. Biol. Chem. **274**: 14255–14261.
25. Zamzami, N., Marchetti, P., Castedi, M., Decaudin, D., Macho, A., Hirsch, T., Susin, S. A., Petit, P. X., Mignotte, B. and Kroemer, G. (1995) Sequential reduction of mitochondrial transmembrane potential and generation of reactive oxygen species in early programmed cell death. J. Exp. Med. **182**: 367–377.
26. Susin, S. A., Lorenzo, H. K., Zamzami, N., Marzo, L., Snow, B. E., Brothers, G. M., Mangion, J., Jacotot, E., Constantini, P., Loeffler, M., Laorochette, N., Goodlett, D. R., Aebersold, R., Siderovski, D., Penninger, J.M. and Kroemer, G. (1999) Molecular characterization of mitochondrial apoptosis-inducing factor. Nature **397**: 441–446.
27. Wang, J. A., Fan, S., Yuan, R. Q., Ma, Y. X., Meng, Q., Goldberg, I. D. and Rosen, E. M. (1999) Ultraviolet radiation down-regulates expression of the cell cycle inhibitor $p21^{WAF1/CIP1}$ in human cancer cells independently of p53. Int. J. Radiat. Biol. **75**: 301–316.
28. Haapajarvi, T., Kivinen, L., Heiskanen, A., des Bordes, C., Datto, M. B., Wang, X. F. and Laiho, M. (1999) UV radiation is a transcriptional inducer of $p21^{Cips/Waf1}$ cyclin-kinase inhibitor in a p53-independent manner. Exp. Cell Res. **248**: 272–279.
29. Finucane, D. M., Waterhouse, N. J., Amarante-Mendes, G. P., Cotter, T. G. and Green, D. R. (1999) Collapse of the inner mitochondrial transmembrane potential is not required for apoptosis of HL60 cells. Exp. Cell Res. **251**: 166–174.
30. Goder, D. E. (1998) UVA1 radiation triggers two different final apoptotic pathways. J. Invest. Dermatol. **112**: 3–12.

31. Rehemtulla, A., Hamilton, C. A., Chinnaiyan, A. M. and Dixit, V. M. (1997) Ultraviolet radiation-induced apoptosis is mediated by activation of CD-95 (Fas/APO-1). J. Biol. Chem. **272**: 25783–25786.
32. Kasibhatla, S. , Brunner, T., Genestier, L., Echeverri, F., Mahboubi, A. Green D.R. (1998) DNA Damaging agents induce expression of Fas ligand and subsequent apoptosis in T lymphcytes via the activation of NF-κB and AP-1. Mol. Cell **1**: 543–551.
33. Bossy-Wetzel, E., Newmeyer, D. D. and Green, D. R. (1998) Mitochondrial cytochrome *c* release in apoptosis occurs upstream of DEVD-specific caspase activation and independently of mitochondrial transmembrane depolarization. EMBO J. **17**: 37–49.
34. Sahara, S., Aoto, M., Eguchi, Y., Imamoto, N., Yoneda, Y. and Tsujimoto, Y. (1999) Acinus is a caspase-3-activated protein required for apoptotic chromatin condensation. Nature **401**: 168–173.
35. Zamzami, N. and Kroemer, G. (1999) Condensed matter in cell death. Nature **401**: 127–128.
36. Hakem, R., Hakem, A., Duncan, G.S., Henderson, J. T., Woo, M., Soengas, M. S. and Elia, A., de la Pompa, J. L., Kagi, D., Kloo, W., Potter, J., Yoshida, R., Kaufmann, S. A., Lowe, S. W., Penninger, J. M. and Mak, T. W. (1998) Differential requirement for caspase 9 in apoptotic pathways *in vivo*. Cell **94**: 339–352.